
Tucker Tensor Layer in Fully Connected Neural Networks

Giuseppe G. Calvi¹ Ahmad Moniri¹ Mahmoud Mahfouz¹ Zeyang Yu¹ Qibin Zhao² Danilo P. Mandic¹

Abstract

We introduce the Tucker Tensor Layer (TTL), an alternative to the dense weight-matrices of the fully connected layers of feed-forward neural networks (NNs), to answer the long standing quest to compress NNs and improve their interpretability. This is achieved by treating these weight-matrices as the unfolding of a higher order weight-tensor. This enables us to introduce a framework for exploiting the multi-way nature of the weight-tensor in order to efficiently reduce the number of parameters, by virtue of the compression properties of tensor decompositions. The Tucker Decomposition (TKD) is employed to decompose the weight-tensor into a core tensor and factor matrices. We re-derive back-propagation within this framework, by extending the notion of matrix derivatives to tensors. In this way, the physical interpretability of the TKD is exploited to gain insights into training, through the process of computing gradients with respect to each factor matrix. The proposed framework is validated on synthetic data and on the Fashion-MNIST dataset, emphasizing the relative importance of various data features in training, hence mitigating the “black-box” issue inherent to NNs. Experiments on both MNIST and Fashion-MNIST illustrate the compression properties of the TTL, achieving a 66.63 fold compression whilst maintaining comparable performance to the uncompressed NN.

1. Introduction

Neural Networks (NNs) are currently the state-of-the-art machine-learning methodology which has delivered improved performance in numerous areas involving large-scale data, such as computer vision, speech recognition, and time-series analysis (LeCun et al., 2015). For example, Recurrent

Neural Networks (RNNs) are among the most successful machine learning approaches when the task is sequence modelling (Graves et al., 2013; Mandic & Chambers, 2001), while Convolutional Neural Networks (CNNs) are well-known to be significantly superior on the task of image classification (Krizhevsky et al., 2012; Simonyan & Zisserman, 2014). Although the theory behind NNs has been established for decades, it was not until recently that they became prominent within the community. Indeed, the application of NNs has also highlighted the necessity of expensive, modern hardware and long processing times, as these models often are composed of thousands of nodes and millions of learning parameters (Russakovsky et al., 2015).

One way to tackle this issue is by employing a tensor approach. Tensors are generalizations of matrices and vectors, which benefit from the power of multilinear algebra to flexibly and efficiently account for multi-way relationships in data while preserving structural information (Cichocki et al., 2015; Kolda & Bader, 2009). Similarly to their matrix counterpart, latent factors in tensors can be extracted via tensor decompositions (TDs); the most commonly used are the Canonical Polyadic (Bro, 1997), the Tensor Train (Oseledets, 2011), and the Tucker (Tucker, 1963) decompositions (CPD, TT, and TKD, respectively). Owing to their compression properties, TDs are just emerging as means to achieve low-rank representations of NNs, by approximating an original network with one having several orders of magnitude fewer parameters, negligibly affecting its overall performance. In (Novikov et al., 2015), the TT format was employed to represent the dense weight matrix of the fully connected layers NNs with only a few parameters. The effectiveness of this approach was demonstrated on standard datasets, on which they achieved high layer compression sacrificing little accuracy. Another approach was taken by (Kossaifi et al., 2017), who proposed the Tensor Contraction Layer (TCL) and Tensor Regression Layer (TRL), to reduce input dimensionality while preserving the tensor multilinear structure, and to express outputs as a mapping between two tensors, respectively. Their work was subsequently extended in (Cao et al., 2017), in which the authors imposed low-rank constraints on the TRL.

Despite these advances, we find that there is still a void in the literature when it comes to deriving back-propagation in terms of tensor latent factors stemming from standard

¹Department of Electrical and Electronic Engineering, Imperial College London, UK ²Laboratory for Advanced Brain Signal Processing, RIKEN, Saitama, Japan. Correspondence to: Giuseppe G. Calvi <ggc115@ic.ac.uk>.

TDs, while at the same time providing physical meaning. For example, although the authors in (Novikov et al., 2015) analytically re-derived back-propagation (Rumelhart et al., 1986) in terms of the TT factors, the dimensionality and order of the employed TTs were arbitrarily chosen, and, while compression was achieved, a physical interpretability of the results was not provided. In this work, we set out to address this void by introducing the Tucker Tensor Layer (TTL), which replaces the dense weight-matrix of a fully connected layer with TKD factors. This is achieved by treating the weight-matrix as the unfolding (flattening) of a higher order weight-tensor. In particular, we focus on the version of TKD named Higher Order Singular Value Decomposition (HOSVD) (Lathauwer et al., 2000), which represents a direct generalization of standard matrix SVD. Due to its uniqueness and ease of interpretability, the HOSVD is a suitable decomposition for obtaining low-rank representations of tensors while at the same time preserving their latent information within their structure.

The goal of this work is therefore to introduce a novel framework for the optimization of NNs through compression of their fully-connected layers, together with increasing interpretability of results by exploiting the desirable properties of TKD. We address the problem from the very core aspects, by fully re-deriving back-propagation from first principles basing our analysis on the fundamentals of vector and matrix derivatives, and extending these to tensors. Next, we provide rigorous mathematical arguments for their manipulation and introduce an analytical formulation of back-propagation in terms of the TKD factors. Moreover, we argue how, by computing the gradient of the loss function with respect to each factor matrix of the TKD, and by keeping track of how they evolve throughout the training phase, we can reveal valuable information on which data features are more important for training, by leveraging on the multi-modal data structure and the expressive power of TKD. This is of high practical importance as it provides insight into how NNs perform their classification, thus mitigating their inherent well-known “black-box” issue. This is illustrated through applications on synthetic and on the Fashion-MNIST datasets. In addition, our proposed framework is further validated by exploring its compressive properties on both MNIST and Fashion-MNIST (LeCun, 1998; Xiao et al., 2017), where in both cases it achieves a 66.63 fold compression while maintaining comparable performance.

2. Notation

Table 1 summarizes the main tensor nomenclature used throughout this work. For more detail, we refer the reader to (Kolda & Bader, 2009; Cichocki et al., 2015; 2016).

Table 1: Main matrix and tensor nomenclature.

$\mathcal{X} \in \mathbb{R}^{I_1 \times I_2 \times \dots \times I_N}$	N -th order tensor of size $I_1 \times I_2 \times \dots \times I_N$
$x_{i_1 i_2 \dots i_N} = \mathcal{X}(i_1, i_2, \dots, i_N)$	(i_1, i_2, \dots, i_N) entry of \mathcal{X}
$x, \mathbf{x}, \mathbf{X}$	Scalar, vector, matrix
$\mathcal{X}^{(n)} \in \mathbb{R}^{I_n \times I_1 I_2 \dots I_{n-1} I_{n+1} \dots I_N}$	Mode- n unfolding of tensor \mathcal{X}
$\mathbf{A}^{(n)}$	Factor matrices
$(\cdot)^T, (\cdot)^{-1}$	Transpose and inverse operators for matrices
\circ, \otimes, \odot	Outer, Kronecker, and Hadamard products
$\text{vec}(\mathcal{X}) = \mathbf{x} \in \mathbb{R}^{I_1 I_2 \dots I_N}$	Vectorization of tensor \mathcal{X}
$\ \cdot\ _F$	Frobenius norm
\mathbf{I}_M	Identity matrix of size $M \times M$
$\mathbf{1}_M$	Vector of ones of size M

3. Theoretical Background

3.1. Tucker Decomposition

The Tucker decomposition (TKD) (Tucker, 1963; 1964) decomposes an N -th order tensor, \mathcal{X} , into a core tensor and N factor matrices. For a 3rd order tensor, the TKD becomes

$$\begin{aligned} \mathcal{X} &\cong \sum_{r_1}^{R_1} \sum_{r_2}^{R_2} \sum_{r_3}^{R_3} g_{r_1 r_2 r_3} \mathbf{u}_{r_1} \circ \mathbf{u}_{r_2} \circ \mathbf{u}_{r_3} \\ &= \mathcal{G} \times_1 \mathbf{U}^{(1)} \times_2 \mathbf{U}^{(2)} \times_3 \mathbf{U}^{(3)} \end{aligned} \quad (1)$$

where $\mathcal{G} \in \mathbb{R}^{R_1 \times R_2 \times R_3}$, and $\mathbf{U}^{(1)} \in \mathbb{R}^{I_1 \times R_1}$, $\mathbf{U}^{(2)} \in \mathbb{R}^{I_2 \times R_2}$, $\mathbf{U}^{(3)} \in \mathbb{R}^{I_3 \times R_3}$, as illustrated in Figure 1.

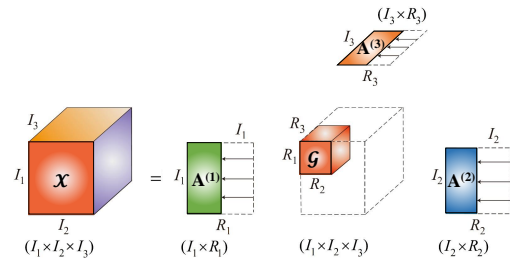


Figure 1: TKD for a 3-rd order tensor $\mathcal{X} \in \mathbb{R}^{I_1 \times I_2 \times I_3}$.

For an N -th order tensor $\mathcal{X} \in \mathbb{R}^{I_1 \times I_2 \times \dots \times I_N}$, the TKD is expressed as

$$\mathcal{X} \cong \mathcal{G} \times_1 \mathbf{U}^{(1)} \times_2 \mathbf{U}^{(2)} \times_3 \dots \times_N \mathbf{U}^{(N)} \quad (2)$$

where $\mathcal{G} \in \mathbb{R}^{R_1 \times R_2 \times \dots \times R_N}$ and $\mathbf{U}^{(n)} \in \mathbb{R}^{I_n \times R_n}$. Throughout this work, significant emphasis is given to the mode- n unfolding of a tensor within the TKD format, that takes the form

$$\begin{aligned} \mathcal{X}_{(n)} = \mathbf{U}^{(n)} \mathcal{G}_{(n)} (\mathbf{U}^{(N)} \otimes \dots \otimes \mathbf{U}^{(n-1)} \otimes \\ \otimes \mathbf{U}^{(n+1)} \otimes \dots \otimes \mathbf{U}^{(1)})^T \end{aligned} \quad (3)$$

while one of the key operators in our analysis is the Kronecker product.

3.2. Properties of the Kronecker Product

If $\mathbf{A} \in \mathbb{R}^{M \times N}$ and $\mathbf{B} \in \mathbb{R}^{P \times Q}$, then the operation $\mathbf{A} \otimes \mathbf{B}$ yields a matrix $\mathbf{C} \in \mathbb{R}^{MP \times NQ}$, with elements $c_{P(r-1)+v, Q(s-1)+w} = a_{rs} b_{vw}$. The Kronecker product is a bilinear and associative operator, non-commutative, and permutation equivalent. Throughout this work, we will mostly use the transpose property of the Kronecker product,

$$(\mathbf{A} \otimes \mathbf{B})^T = \mathbf{A}^T \otimes \mathbf{B}^T \quad (4)$$

and the following identity

$$\text{vec}(\mathbf{AXB}) = (\mathbf{B}^T \otimes \mathbf{A}) \text{vec}(\mathbf{X}) \quad (5)$$

4. Tensor Derivatives

A prerequisite in our approach is to extend the notion of vector and matrix derivatives to higher-order tensors. We base our analysis on reformulations of Definition 4 and Definition 6 in (Magnus & Neudecker, 1985).

Definition 1. A ball in $\mathbb{R}^{I_1 \times I_2 \times \dots \times I_N}$ of radius r is denoted by

$$B(\mathcal{C}; r) = \{\mathcal{X} : \mathcal{X} \in \mathbb{R}^{I_1 \times I_2 \times \dots \times I_N}, \|\mathcal{X} - \mathcal{C}\|_F < r\} \quad (6)$$

where $\mathcal{C} \in \mathbb{R}^{I_1 \times I_2 \times \dots \times I_N}$ is an interior point of a set S in $\mathbb{R}^{I_1 \times I_2 \times \dots \times I_N}$.

Definition 2. Let S be a set in $\mathbb{R}^{I_1 \times I_2 \times \dots \times I_N}$, and let $F : S \mapsto \mathbb{R}^{J_1 \times J_2 \times \dots \times J_M}$ be a tensor function operating on S . Notice that $N \neq M$, i.e. F does not necessarily map a tensor to a tensor of the same order. Let the tensor $\mathcal{C} \in \mathbb{R}^{I_1 \times I_2 \times \dots \times I_N}$ be an interior point of S , and let $B(\mathcal{C}; r) \subset S$ be a ball with centre \mathcal{C} and radius r . Let \mathcal{E} be an arbitrary tensor in $\mathbb{R}^{I_1 \times I_2 \times \dots \times I_N}$, with $\|\mathcal{E}\|_F < r$, so that $(\mathcal{C} + \mathcal{E}) \in B(\mathcal{C}; r)$. If there exist a matrix $\mathbf{A} \in \mathbb{R}^{J_1 J_2 \dots J_M \times I_1 I_2 \dots I_N}$, which depends on \mathcal{C} but not on \mathcal{E} , so that

$$\text{vec}(F(\mathcal{C} + \mathcal{E})) = \text{vec}(F(\mathcal{C})) + \mathbf{A}(\mathcal{C}) \text{vec}(\mathcal{E}) + \text{vec}(R_{\mathcal{C}}(\mathcal{E})) \quad (7)$$

for all $\mathcal{E} \in \mathbb{R}^{I_1 \times I_2 \times \dots \times I_N}$ with $\|\mathcal{E}\|_F < r$, where the remainder $R_{\mathcal{C}}(\mathcal{E})$ is of a smaller order than $\|\mathcal{E}\|_F$ as $\mathcal{E} \rightarrow 0$, that is

$$\lim_{\mathcal{E} \rightarrow 0} \frac{R_{\mathcal{C}}(\mathcal{E})}{\|\mathcal{E}\|_F} = 0 \quad (8)$$

then the function F is said to be *differentiable* at \mathcal{C} . The matrix $dF(\mathcal{C}; \mathcal{E}) \in \mathbb{R}^{J_1 \times J_2 \times \dots \times J_M}$ is defined by

$$\text{vec}(dF(\mathcal{C}; \mathcal{E})) = \mathbf{A}(\mathcal{C}) \text{vec}(\mathcal{E}) \quad (9)$$

then called the *first differential of F at \mathcal{C} with increment \mathcal{E}* .

Similarly as with the matrix case, in view of Definition 2, the calculus properties of vector functions can be readily extended to tensors, because, instead of considering the tensor function $F : S \mapsto \mathbb{R}^{J_1 \times J_2 \times \dots \times J_M}$, we consider the vector function $f : \text{vec}(S) \mapsto \mathbb{R}^{J_1 J_2 \dots J_M \times 1}$ defined by

$$f(\text{vec}(\mathcal{X})) = \text{vec}(F(\mathcal{X})) \quad (10)$$

As a result it follows that

$$\text{vec}(dF(\mathcal{C}; \mathcal{E})) = df(\text{vec}(\mathcal{C}); \text{vec}(\mathcal{E})) \quad (11)$$

This justifies the following definition.

Definition 3. Consider a tensor $\mathcal{X} \in \mathbb{R}^{I_1 \times I_2 \times \dots \times I_N}$ and the differentiable tensor function $F : \mathcal{X} \mapsto \mathbb{R}^{J_1 \times J_2 \times \dots \times J_M}$. Then, the matrix in $\mathbb{R}^{J_1 J_2 \dots J_M \times I_1 I_2 \dots I_N}$

$$\frac{\partial F(\mathcal{X})}{\partial \mathcal{X}} = D(F(\mathcal{X})) = Df(\text{vec}(\mathcal{X})) = \frac{\partial f(\text{vec}(\mathcal{X}))}{\partial \text{vec}(\mathcal{X})} \quad (12)$$

is called the *derivative of F at \mathcal{X}* .

A special case of Definition 3 is found when the input to a tensor function is a matrix, as formalized in the following definition.

Definition 4. Consider a matrix $\mathbf{X} \in \mathbb{R}^{M \times P}$ and the differentiable tensor function $F : \mathbf{X} \mapsto \mathbb{R}^{I_1 \times I_2 \times \dots \times I_N}$. Then the matrix in $\mathbb{R}^{I_1 I_2 \dots I_N \times MP}$, given by

$$\frac{\partial F(\mathbf{X})}{\partial \mathbf{X}} = D(F(\mathbf{X})) = Df(\text{vec}(\mathbf{X})) = \frac{\partial f(\text{vec}(\mathbf{X}))}{\partial \text{vec}(\mathbf{X})} \quad (13)$$

is called the *derivative or Jacobian of F at \mathbf{X}* .

Given the above definitions, we are now equipped to propose the next theorem.

Theorem 1. Consider a matrix $\mathbf{X} \in \mathbb{R}^{M \times P}$ and the differentiable tensor function $F : \mathbf{X} \mapsto \mathbb{R}^{I_1 \times I_2 \times \dots \times I_N}$. Let $\mathcal{Y} = F(\mathcal{X})$, and $\mathcal{Y}_{(n)}$ be the mode- n unfolding of \mathcal{Y} . Then $\forall n \in \{1, 2, \dots, N\}$, $D(\mathcal{Y}_{(n)})$ is a permuted version of $D(\mathcal{Y}) = D(F(\mathcal{X}))$, i.e. $D(\mathcal{Y})$ and $D(\mathcal{Y}_{(n)})$ are matrices containing the same elements, but arranged differently. We can write this as

$$D(\mathcal{Y}_{(n)}) = \mathcal{P}(D(\mathcal{Y})) \quad (14)$$

where \mathcal{P} is a permutation operator.

Proof. Let $\mathbf{X} \in \mathbb{R}^{M \times P}$ and $\mathcal{Y} = F(\mathbf{X}) \in \mathbb{R}^{I_1 \times I_2 \times \dots \times I_N}$. From Definition 4 and Equation 13 we have

$$D(\mathcal{Y}) = \frac{\partial \mathcal{Y}}{\partial \mathbf{X}} = \frac{\partial \text{vec}(\mathcal{Y})}{\partial \text{vec}(\mathbf{X})} \in \mathbb{R}^{I_1 I_2 \dots I_N \times MP} \quad (15)$$

At the same time, this results in $\mathcal{Y}_{(n)} \in \mathbb{R}^{I_n \times I_1 I_2 \dots I_{n-1} I_{n+1} \dots I_N}$. Next, from Definition 4 and Equation 13 we obtain

$$D(\mathcal{Y}_{(n)}) = \frac{\partial \mathcal{Y}_{(n)}}{\partial \mathbf{X}} = \frac{\partial \text{vec}(\mathcal{Y}_{(n)})}{\partial \text{vec}(\mathbf{X})} \in \mathbb{R}^{I_n I_1 \dots I_{n-1} I_{n+1} \dots I_N \times MP} \quad (16)$$

Hence, $D(\mathcal{Y})$ and $D(\mathcal{Y}_{(n)})$ have the same dimensionality. Because $\text{vec}(\mathcal{Y})$ and $\text{vec}(\mathcal{Y}_{(n)})$ clearly have the same elements but arranged differently, $D(\mathcal{Y}_{(n)})$ is a permuted version of $D(\mathcal{Y})$. \square

Corollary 1. Consider a matrix $\mathbf{X} \in \mathbb{R}^{M \times P}$ and the differentiable tensor function $F : \mathbf{X} \mapsto \mathbb{R}^{I_1 \times I_2 \times \dots \times I_N}$. Let $\mathcal{Y} = F(\mathbf{X})$, and let $\mathcal{Y}_{(n)}$ and $\mathcal{Y}_{(m)}$ be respectively the mode- n and mode- m unfoldings of \mathcal{Y} . Then $D(\mathcal{Y}_{(n)})$ and $D(\mathcal{Y}_{(m)})$ are of the same dimensionality, but with permuted elements. This can be written as

$$D(\mathcal{Y}_{(n)}) = \mathcal{P}(D(\mathcal{Y}_{(m)})) \quad (17)$$

where \mathcal{P} is a permutation operator.

Proof. Follows immediately from Theorem 1. \square

5. Tucker Tensor Layer

5.1. Representation

To introduce the Tucker Tensor Layer (TTL), observe that, in general, a fully connected layer within a NN can be expressed as (here we do not consider non-linearities for simplicity, although they are included in later sections)

$$\mathbf{y} = \mathbf{W}\mathbf{x} + \mathbf{b} \quad (18)$$

where $\mathbf{y} \in \mathbb{R}^M$ is the output, $\mathbf{x} \in \mathbb{R}^N$ the input, and $\mathbf{W} \in \mathbb{R}^{M \times N}$ is the connecting matrix of weights. Now, consider an input tensor of order N , $\mathcal{X} \in \mathbb{R}^{I_1 \times I_2 \times \dots \times I_N}$, and a weight tensor $\mathcal{W} \in \mathbb{R}^{I_1 \times I_2 \times \dots \times I_{N+1}}$, of order $N+1$. We shall investigate the function $F : \mathcal{X} \mapsto \mathbb{R}^{I_{N+1}}$, where I_{N+1} is the number of classes, defined by

$$F(\mathcal{X}) = \mathcal{W}_{(N+1)} \text{vec}(\mathcal{X}) + \mathbf{b} \quad (19)$$

where $\mathbf{b} \in \mathbb{R}^{I_{N+1}}$ is a bias vector, $\mathcal{W}_{(N+1)} \in \mathbb{R}^{I_{N+1} \times I_1 I_2 \dots I_N}$ is the $(N+1)$ -mode unfolding of tensor \mathcal{W} , and $\text{vec}(\mathcal{X}) \in \mathbb{R}^{I_1 I_2 \dots I_N}$ is the vectorization of tensor \mathcal{X} . In (19) we have set $\mathbf{y} = F(\mathcal{X})$, $\mathbf{W} = \mathcal{W}_{(N+1)}$, and $\mathbf{x} = \text{vec}(\mathcal{X})$. As we shall show in the following, representation (19) has the advantage of allowing a compressed version of the NN layer, via tensor decompositions.

A tensor \mathcal{W} can be represented in the TKD format as

$$\mathcal{W} = \mathcal{G} \times_1 \mathbf{U}^{(1)} \times_2 \mathbf{U}^{(2)} \times \dots \times_{N+1} \mathbf{U}^{(N+1)} \quad (20)$$

where $\mathcal{G} \in \mathbb{R}^{R_1 \times R_2 \times \dots \times R_{N+1}}$ is the core tensor, and $\mathbf{U}^{(n)} \in \mathbb{R}^{I_n \times R_n}$ the corresponding factor matrices. This implies that the $(N+1)$ -mode unfolding of \mathcal{W} , denoted by $\mathcal{W}_{(N+1)}$, can be expressed as

$$\begin{aligned} \mathcal{W}_{(N+1)} &= \mathbf{U}^{(N+1)} \mathcal{G}_{(N+1)} (\mathbf{U}^{(N)} \otimes \dots \otimes \mathbf{U}^{(1)})^T \\ &= \mathbf{U}^{(N+1)} \mathcal{G}_{(N+1)} \bigotimes_{i=N}^1 \mathbf{U}^{(i)T} \end{aligned} \quad (21)$$

Upon substituting (21) into (19) we have

$$F(\mathcal{X}) = \left[\mathbf{U}^{(N+1)} \mathcal{G}_{(N+1)} \bigotimes_{i=N}^1 \mathbf{U}^{(i)T} \right] \text{vec}(\mathcal{X}) + \mathbf{b} \quad (22)$$

Remark 1. The compression of the NN is achieved through the TTL, by selecting the size of the modes of core \mathcal{G} to be smaller than those of \mathcal{W} , that is $R_n < I_n$, for $n = 1, 2, \dots, N+1$.

5.2. Learning via Back-propagation

Neural networks are generally trained with stochastic gradient descent algorithms, where at each step the gradient is computed using the back-propagation procedure (Rumelhart et al., 1986). It starts by computing the gradient of a loss function L w.r.t. the output, then proceeds sequentially through the layers of the NN, but in a reversed order. When applied to the fully connected layer as expressed in (19), given the gradient $\frac{\partial L}{\partial F(\mathcal{X})}$, back-propagation computes (Novikov et al., 2015)

$$\begin{aligned} \frac{\partial L}{\partial \text{vec}(\mathcal{X})} &= \mathcal{W}_{(N+1)}^T \frac{\partial L}{\partial F(\mathcal{X})} \\ \frac{\partial L}{\partial \mathbf{b}} &= \frac{\partial L}{\partial F(\mathcal{X})} \\ \frac{\partial L}{\partial \mathcal{W}_{(N+1)}} &= \frac{\partial L}{\partial F(\mathcal{X})} \text{vec}(\mathcal{X})^T \end{aligned} \quad (23)$$

Since L is a scalar, the gradients in (23) are of dimensionality $\frac{\partial L}{\partial \text{vec}(\mathcal{X})} \in \mathbb{R}^{I_1 I_2 \dots I_N}$, $\frac{\partial L}{\partial \mathbf{b}} \in \mathbb{R}^{I_{N+1}}$, and $\frac{\partial L}{\partial \mathcal{W}_{(N+1)}} \in \mathbb{R}^{I_{N+1} \times I_1 I_2 \dots I_N}$. This allows, at each iteration, to update the weight matrix as $\mathcal{W}_{(N+1)t+1} = \mathcal{W}_{(N+1)t} + \mu \frac{\partial L}{\partial \mathcal{W}_{(N+1)t}}$ where μ is a step size.

To derive backpropagation based on the Tucker model in (20), first consider that the gradient $\frac{\partial L}{\partial \mathbf{U}^{(n)}}$ is a function of $\frac{\partial L}{\partial F(\mathcal{X})}$, $\frac{\partial F(\mathcal{X})}{\partial \mathcal{W}_{(N+1)}}$, $\frac{\partial \mathcal{W}_{(N+1)}}{\partial \mathbf{U}^{(n)}}$, that is

$$\frac{\partial L}{\partial \mathbf{U}^{(n)}} = \Omega \left(\frac{\partial L}{\partial F(\mathcal{X})}, \frac{\partial F(\mathcal{X})}{\partial \mathcal{W}_{(N+1)}}, \frac{\partial \mathcal{W}_{(N+1)}}{\partial \mathbf{U}^{(n)}} \right) \quad (24)$$

Then, define the following shorthand notation for dimensionalities: $\underline{R}_{-n} = R_1 R_2 \dots R_{n-1} R_{n+1} \dots R_{N+1}$, $\underline{I}_{-n} = I_1 I_2 \dots I_{n-1} I_{n+1} \dots I_{N+1}$, $\underline{I}_N = I_1 I_2 \dots I_N$ and $\underline{I}_{N+1} = I_1 I_2 \dots I_{N+1}$. From the rules of the Kronecker product, we now obtain

$$\frac{\partial F(\mathcal{X})}{\partial \mathcal{W}_{(N+1)}} = \text{vec}(\mathcal{X})^T \otimes \mathbf{I}_{I_{N+1}} \in \mathbb{R}^{I_{N+1} \times I_{N+1}} \quad (25)$$

At this stage, a closer inspection of equation (24) is required. Consider $\frac{\partial \mathcal{W}_{(N+1)}}{\partial \mathbf{U}^{(n)}} \in \mathbb{R}^{I_{N+1} \times R_n I_n}$. By Corollary 1, this matrix can be found as a permutation of $\frac{\partial \mathcal{W}_{(n)}}{\partial \mathbf{U}^{(n)}}$, which is a matrix of the same dimensionality and containing the same elements. In other words,

$$\frac{\partial \mathcal{W}_{(N+1)}}{\partial \mathbf{U}^{(n)}} = \mathcal{P} \left(\frac{\partial \mathcal{W}_{(n)}}{\partial \mathbf{U}^{(n)}} \right) = \mathbf{P}_n \frac{\partial \mathcal{W}_{(n)}}{\partial \mathbf{U}^{(n)}} \quad (26)$$

where $\mathbf{P}_n \in \mathbb{R}^{I_{N+1} \times I_{N+1}}$ is a permutation matrix that satisfies

$$\text{vec}(\mathcal{W}_{(n)}) = \mathbf{P}_n \text{vec}(\mathcal{W}_{(N+1)}) \quad (27)$$

The task hence becomes to compute

$$\frac{\partial L}{\partial \mathbf{U}^{(n)}} = \Omega \left(\frac{\partial L}{\partial F(\mathcal{X})}, \frac{\partial F(\mathcal{X})}{\partial \mathcal{W}_{(N+1)}}, \mathbf{P}_n \frac{\partial \mathcal{W}_{(n)}}{\partial \mathbf{U}^{(n)}} \right) \quad (28)$$

The mode- n unfolding of the weight tensor $\mathcal{W} \in \mathbb{R}^{I_1 \times I_2 \times \dots \times I_{N+1}}$ is given by

$$\begin{aligned} \mathcal{W}_{(n)} &= \mathbf{U}^{(n)} \mathcal{G}_{(n)} (\mathbf{U}^{(N+1)} \otimes \dots \otimes \\ &\quad \otimes \mathbf{U}^{(n+1)} \otimes \mathbf{U}^{(n-1)} \otimes \dots \otimes \mathbf{U}^{(1)})^T \\ &= \mathbf{U}^{(n)} \mathcal{G}_{(n)} \bigotimes_{\substack{i=N+1 \\ i \neq n}}^1 \mathbf{U}^{(i)T} \in \mathbb{R}^{I_n \times I_{-n}} \end{aligned} \quad (29)$$

while its partial derivative w.r.t. $\mathbf{U}^{(n)}$ now becomes

$$\begin{aligned} \frac{\partial \mathcal{W}_{(n)}}{\partial \mathbf{U}^{(n)}} &= (\mathbf{U}^{(N+1)} \otimes \dots \otimes \\ &\quad \otimes \mathbf{U}^{(n+1)} \otimes \mathbf{U}^{(n-1)} \otimes \dots \otimes \mathbf{U}^{(1)}) \mathcal{G}_{(n)}^T \otimes \mathbf{I}_{I_n} \\ &= \bigotimes_{\substack{i=N+1 \\ i \neq n}}^1 \mathbf{U}^{(i)} \mathcal{G}_{(n)}^T \otimes \mathbf{I}_{I_n} \in \mathbb{R}^{I_{N+1} \times R_n I_n} \end{aligned} \quad (30)$$

From (24) we require $\frac{\partial L}{\partial \mathbf{U}^{(n)}} \in \mathbb{R}^{I_n \times R_n}$, which is the matricization of $\frac{\partial L}{\partial \text{vec}(\mathbf{U}^{(n)})} \in \mathbb{R}^{R_n I_n}$. Therefore, to find $\frac{\partial L}{\partial \mathbf{U}^{(n)}} \in \mathbb{R}^{I_n \times R_n}$, it is sufficient to compute $\frac{\partial L}{\partial \text{vec}(\mathbf{U}^{(n)})} \in \mathbb{R}^{R_n I_n}$ and reshape the result accordingly. Since $\frac{\partial L}{\partial F(\mathcal{X})} \in \mathbb{R}^{I_{N+1}}$, $\frac{\partial F(\mathcal{X})}{\partial \mathcal{W}_{(N+1)}} \in \mathbb{R}^{I_{N+1} \times I_{N+1}}$, $\frac{\partial \mathcal{W}_{(n)}}{\partial \mathbf{U}^{(n)}} \in \mathbb{R}^{I_{N+1} \times R_n I_n}$ and $\frac{\partial L}{\partial \text{vec}(\mathbf{U}^{(n)})} \in \mathbb{R}^{R_n I_n}$, this results in

$$\frac{\partial L}{\partial \text{vec}(\mathbf{U}^{(n)})} = \left(\mathbf{P}_n \frac{\partial \mathcal{W}_{(n)}}{\partial \mathbf{U}^{(n)}} \right)^T \frac{\partial F(\mathcal{X})}{\partial \mathcal{W}_{(N+1)}}^T \frac{\partial L}{\partial F(\mathcal{X})} \quad (31)$$

Similarly, since $\frac{\partial L}{\partial \mathcal{G}_{(N+1)}} \in \mathbb{R}^{R_{N+1} \times R_N}$ can be computed by considering $\frac{\partial L}{\partial \text{vec}(\mathcal{G}_{(N+1)})} \in \mathbb{R}^{R_{N+1}}$, we arrive at

$$\frac{\partial L}{\partial \text{vec}(\mathcal{G}_{(N+1)})} = \frac{\partial \mathcal{W}_{(N+1)}}{\partial \mathcal{G}_{(N+1)}}^T \frac{\partial F(\mathcal{X})}{\partial \mathcal{W}_{(N+1)}}^T \frac{\partial L}{\partial F(\mathcal{X})} \quad (32)$$

where

$$\frac{\partial \mathcal{W}_{(N+1)}}{\partial \mathcal{G}_{(N+1)}} = (\mathbf{U}^{(N)} \otimes \dots \otimes \mathbf{U}^{(1)}) \otimes \mathbf{U}^{(N+1)} \in \mathbb{R}^{I_{N+1} \times R_{N+1}} \quad (33)$$

6. Algorithm Implementation

To illustrate the algorithmic implementation of the results obtained in Section 5, we consider a dataset consisting of N -th order tensors $\mathcal{X} \in \mathbb{R}^{I_1 \times I_2 \times \dots \times I_N}$ and their corresponding labels, that is $\{\mathcal{X}_m, y_m\}_m^M$, $m = 1, \dots, M$, where M is the size of the dataset. For an efficient representation, the data is organized in a matrix $\underline{\mathbf{X}} \in \mathbb{R}^{I_N \times M}$, defined as

$$\underline{\mathbf{X}} = [\text{vec}(\mathcal{X}_1), \text{vec}(\mathcal{X}_2), \dots, \text{vec}(\mathcal{X}_M)] \quad (34)$$

so that Equation (19) can be re-written as

$$F(\underline{\mathbf{X}}) = \mathcal{W}_{(N+1)} \underline{\mathbf{X}} + \mathbf{B} \quad (35)$$

where $\mathbf{B} \in \mathbb{R}^{I_{N+1} \times M}$ is a matrix of biases, and $F(\underline{\mathbf{X}}) \in \mathbb{R}^{I_{N+1} \times M}$. Note that $\mathbf{B}^{(l)} \in \mathbb{R}^{I_{N+1}^{(l)} \times M}$ must apply the same biases to each element in the dataset, and, as such, has the structure of $\mathbf{B}^{(l)} = \mathbf{b}^{(l)} \mathbf{1}_M^T$

$$\mathbf{B}^{(l)} = \mathbf{b}^{(l)} \mathbf{1}_M^T \quad (36)$$

where $\mathbf{b}^{(l)} \in \mathbb{R}^{I_{N+1}^{(l)}}$ are the actual biases.

Consider now a neural network composed of layers indexed by $l = 0, 1, 2, \dots, L$, where $l = 0$ is the input layer, $l = L$ is the output layer, and $l = 1, \dots, L - 1$ are the hidden layers. For generality, assume that all layers are TTLs. Slightly modifying our notation, for each layer we denote inputs and outputs as summarized in Table 2.

Upon calculating the gradient of the cost function L w.r.t the input of the last layer of the network $\underline{\mathbf{Z}}^{(L)}$, that is $\frac{\partial L}{\partial \underline{\mathbf{F}}^{(L)}} \in \mathbb{R}^{I_{N+1}^{(L)} \times M}$, the error is then back-propagated through layers $l = L - 1, L - 2, \dots, 1$. As a result the gradients of the cost function w.r.t. the factor matrices and the core tensor of the l -th Tucker tensor layer are computed as

$$\begin{aligned} \frac{\partial L}{\partial \text{vec}(\mathbf{U}^{(n)})} &= \left(\mathbf{P}_n \frac{\partial \mathcal{W}_{(n)}^{(l)}}{\partial \mathbf{U}^{(n)}} \right)^T \frac{\partial \underline{\mathbf{F}}^{(l)}}{\partial \mathcal{W}_{(N+1)}^{(l)}}^T \text{vec}(\underline{\mathbf{D}}^{(l)}) \\ \frac{\partial L}{\partial \text{vec}(\mathcal{G}_{(N+1)}^{(l)})} &= \frac{\partial \mathcal{W}_{(N+1)}^{(l)}}{\partial \mathcal{G}_{(N+1)}^{(l)}}^T \frac{\partial \underline{\mathbf{F}}^{(l)}}{\partial \mathcal{W}_{(N+1)}^{(l)}}^T \text{vec}(\underline{\mathbf{D}}^{(l)}) \end{aligned} \quad (37)$$

Table 2: Inputs and outputs of network layers.

$\underline{\mathbf{Z}}^{(0)} = \underline{\mathbf{X}}$	Output of layer $l = 0$: the input to the network
$\mathcal{W}_{(N+1)}^{(l)}$	Weight matrix for layers $l = 1, \dots, L$
$\mathbf{U}_{(l)}^{(n)}, \mathcal{G}_{(N+1)}^{(l)}$	Factor matrices and core tensor associated to $\mathcal{W}_{(N+1)}^{(l)}$ for layers $l = 1, \dots, L$
$\underline{\mathbf{F}}^{(l)} = \mathcal{W}_{(N+1)}^{(l)} \underline{\mathbf{Z}}^{(l-1)} + \mathbf{B}^{(l)}$	Input to layers $l = 1, \dots, L$
$\underline{\mathbf{Z}}^{(l)} = \sigma(\underline{\mathbf{F}}^{(l)})$	Output of layers $l = 1, \dots, L$, where $\sigma(\cdot)$ is a point-wise activation function

where

$$\underline{\mathbf{D}}^{(l)} = \begin{cases} \frac{\partial L}{\partial \underline{\mathbf{Z}}^{(L)}} \frac{\partial \underline{\mathbf{Z}}^{(L)}}{\partial \underline{\mathbf{F}}^{(L)}} = \frac{\partial L}{\partial \underline{\mathbf{F}}^{(L)}}, & \text{if } l = L \\ \mathcal{W}_{(N+1)}^{(l+1)T} \underline{\mathbf{D}}^{(l+1)} \odot \sigma'(\underline{\mathbf{F}}^{(l)}), & \text{if } l = L-1, \dots, 1 \end{cases} \quad (38)$$

and

$$\frac{\partial \underline{\mathbf{F}}^{(l)}}{\partial \mathcal{W}_{(N+1)}^{(l)}} = \underline{\mathbf{Z}}^{(l-1)T} \otimes \mathbf{I}_{I_{N+1}}^{(l)} \quad (39)$$

By substituting Equations (33) and (39) into Equation (37), we can now rewrite the gradients for the factor matrices $\mathbf{U}_{(l)}^{(n)}$ and the core tensors $\mathcal{G}_{(N+1)}^{(l)}$ as

$$\begin{aligned} \frac{\partial L}{\partial \text{vec}(\mathbf{U}_{(l)}^{(n)})} &= \left(\mathbf{P}_n \frac{\partial \mathcal{W}_{(N+1)}^{(l)}}{\partial \mathbf{U}_{(l)}^{(n)}} \right)^T \text{vec}(\underline{\mathbf{D}}^{(l)} \underline{\mathbf{Z}}^{(l-1)T}) \\ \frac{\partial L}{\partial \mathcal{G}_{(N+1)}^{(l)}} &= \mathbf{U}_{(l)}^{(N+1)T} \underline{\mathbf{D}}^{(l)} \underline{\mathbf{Z}}^{(l-1)T} \left(\bigotimes_{i=N}^1 \mathbf{U}_{(l)}^{(i)} \right) \end{aligned} \quad (40)$$

Moreover, if $n = N + 1$, by making use of Equation (30), we directly obtain the result

$$\frac{\partial L}{\partial \mathbf{U}_{(l)}^{(N+1)}} = \underline{\mathbf{D}}^{(l)} \underline{\mathbf{Z}}^{(l-1)T} \left(\bigotimes_{i=N}^1 \mathbf{U}_{(l)}^{(i)} \right) \mathcal{G}_{(N+1)}^{(l)T} \quad (41)$$

Similarly, $\frac{\partial L}{\partial \mathbf{b}^{(l)}} \in \mathbb{R}^{I_{N+1}^{(l)}}$ can be computed first by considering $\frac{\partial L}{\partial \mathbf{B}^{(l)}} \in \mathbb{R}^{I_{N+1}^{(l)} \times M}$,

$$\begin{aligned} \frac{\partial L}{\partial \text{vec}(\mathbf{B}^{(l)})} &= \frac{\partial \underline{\mathbf{F}}^{(l)}}{\partial \mathbf{B}^{(l)}} \text{vec}(\underline{\mathbf{D}}^{(l)}) \\ &= (\mathbf{I}_M \otimes \mathbf{I}_{I_{N+1}}^{(l)}) \text{vec}(\underline{\mathbf{D}}^{(l)}) \end{aligned} \quad (42)$$

Algorithm 1 Forward and back-propagation for TTLs

```

1: Input: Dataset  $\underline{\mathbf{X}} \in \mathbb{R}^{I_N \times M}$ 
2:
3:  $\underline{\mathbf{Z}}^{(0)} = \underline{\mathbf{X}}$ , and initialize all  $\mathbf{U}_{(l)}^{(n)}$  and  $\mathcal{G}_{(N+1)}^{(l)}$ 
4:
5: Forward propagation:
6: for  $l = 1, \dots, L$  do
7:   Compute  $\mathcal{W}_{(N+1)}^{(l)}$  via Equation (21)
8:    $\underline{\mathbf{F}}^{(l)} = \mathcal{W}_{(N+1)}^{(l)} \underline{\mathbf{Z}}^{(l-1)} + \mathbf{B}^{(l)}$ 
9:    $\underline{\mathbf{Z}}^{(l)} = \sigma(\underline{\mathbf{F}}^{(l)})$ 
10:  Store  $\underline{\mathbf{F}}^{(l)}, \underline{\mathbf{Z}}^{(l)}$ 
11:  Compute and store  $\sigma'(\underline{\mathbf{F}}^{(l)})$ 
12: end for
13:
14: Backpropagation:
15: for  $l = L, L-1, \dots, 1$  do
16:  Compute  $\underline{\mathbf{D}}^{(l)}$  via Equation (38)
17:  Compute the gradients via Equations (40)-(43)
18:   $\mathbf{U}_{(l)}^{(n)} \leftarrow \mathbf{U}_{(l)}^{(n)} - \eta \left( \frac{\partial L}{\partial \mathbf{U}_{(l)}^{(n)}} \right)$ 
19:   $\mathcal{G}_{(N+1)}^{(l)} \leftarrow \mathcal{G}_{(N+1)}^{(l)} - \eta \left( \frac{\partial L}{\partial \mathcal{G}_{(N+1)}^{(l)}} \right)$ 
20:   $\mathbf{b}^{(l)} \leftarrow \mathbf{b}^{(l)} - \eta \left( \frac{\partial L}{\partial \mathbf{b}^{(l)}} \right)$ 
21: end for

```

Hence, from the rules of the Kronecker product, $\frac{\partial L}{\partial \mathbf{B}^{(l)}} = \underline{\mathbf{D}}^{(l)}$, which implies that,

$$\begin{aligned} \frac{\partial L}{\partial \mathbf{b}^{(l)}} &= \left(\frac{\partial \mathbf{B}^{(l)}}{\partial \mathbf{b}^{(l)}} \right)^T \text{vec}(\underline{\mathbf{D}}^{(l)}) \\ &= \left(\mathbf{1}_M^T \otimes \mathbf{I}_{I_{N+1}}^{(l)} \right) \text{vec}(\underline{\mathbf{D}}^{(l)}) \end{aligned} \quad (43)$$

The forward and back-propagation procedures are summarized in Algorithm 1 and implemented using the freely available Higher Order Tensor ToolBOX (HOTTBOX) (Kisil et al.).

7. Simulation Results

7.1. Physical Interpretability

Recall that Equation (22) is the general equation for the TTL model. It is therefore natural to ask whether the matrices $\mathbf{U}^{(n)} \in \mathbb{R}^{I_n \times R_n}$ are physically related to the data tensors $\mathcal{X} \in \mathbb{R}^{I_1 \times I_1 \times \dots \times I_N}$. Consider the identity,

$$\begin{aligned} F(\mathcal{X}) &= \left[\mathbf{U}^{(N+1)} \mathcal{G}_{(N+1)} \bigotimes_{i=N}^1 \mathbf{U}^{(i)T} \right] \text{vec}(\mathcal{X}) + \mathbf{b} \\ &= \mathbf{U}^{(N+1)} \mathcal{G}_{(N+1)} \text{vec}(\mathcal{X} \times_1 \mathbf{U}^{(1)T} \times_2 \\ &\quad \times_2 \mathbf{U}^{(2)T} \times \dots \times_N \mathbf{U}^{(N)T}) + \mathbf{b} \end{aligned} \quad (44)$$

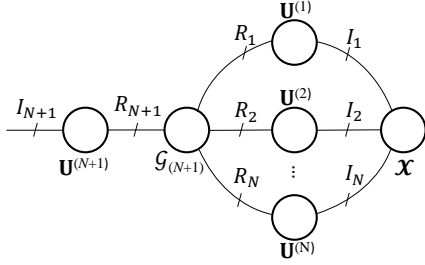


Figure 2: **Graphical representation of Equation (44).**

Remark 2. This implies that the n physical modes, of dimensionality I_n , of tensors \mathcal{X} are directly intertwined with the corresponding factor matrices $\mathbf{U}^{(n)}$. As a direct consequence, certain gradient terms $\frac{\partial L}{\partial \mathbf{U}^{(n)}}$ will carry more significant information than others, depending on which modes I_n of the original data tensors are richer in structure. This is of great importance, as one of the most well-known problems with NNs is their black-box nature, while the proposed method offers viable means to aid understanding which data features have a higher influence on their training process.

Figure 2 offers a graphical representation of Equation (44). Each node represents a tensor, the order of which is determined by the number of edges it connects to. The edges represent the modes, and their labels the corresponding dimensionality.

Remark 3. From Figure 2, it becomes apparent that each factor matrix, $\mathbf{U}^{(n)}$, and hence each gradient, $\frac{\partial L}{\partial \mathbf{U}^{(n)}}$, is associated with the respective mode- n , suggesting that the gradients themselves will carry valuable information related to the underlying data structure.

7.2. Synthetic Data

To provide more intuition into the above discussion, we evaluated our model on two synthetic datasets, referred to as Synthetic Dataset 1 (SD1), and Synthetic Dataset 2 (SD2). Each dataset is composed of 28×28 grey-scale images (2-nd order tensors), which are white everywhere except at randomly selected rows for SD1 and randomly selected columns for SD2, which are black. Examples of images from said datasets are shown in Figure 3.

Such a structure was chosen for SD1 and SD2 to ensure that one tensor mode is far richer in structure than the other. It is expected that $\frac{\partial L}{\partial \mathbf{U}^{(1)}}$ will be more important than $\frac{\partial L}{\partial \mathbf{U}^{(2)}}$ for SD1, and vice-versa for SD2. For quantitative assessment, at each epoch we stored the normalized Frobenius norm of each gradient, defined as $\frac{\partial L^*}{\partial \mathbf{U}^{(n)}} = \left\| \frac{\partial L}{\partial \mathbf{U}^{(n)}} \right\|_F / (I_n R_n)$.

Simulations were run for 50 epochs and the results are shown in the left-most column of Figure 4, which suggest that the proposed model is capable of capturing well the

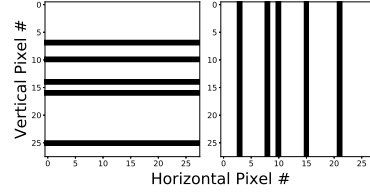


Figure 3: **Sample images from two synthetic datasets.** *Left:* Synthetic Dataset 1. *Right:* Synthetic Dataset 2.

relative importance of the modal structure within data. In the case of SD1, mode-1 is richer in structure, and this is indicated by the fact that $\frac{\partial L^*}{\partial \mathbf{U}^{(1)}} > \frac{\partial L^*}{\partial \mathbf{U}^{(2)}}$ for all epochs. The converse is true for SD2. This demonstrates that the TTL implicitly resolves the notorious black-box nature of NNs, by offering physically meaningful information inferred from the gradients of the trained weights.

7.3. MNIST

We now demonstrate the desirable compression properties of the TTL by applying it to the MNIST dataset (LeCun, 1998) for the task of handwritten digit recognition. The MNIST dataset is composed of 50000 28×28 greyscale images for training, 10000 for validation purposes, and 10000 for testing. We used a neural network with 1 hidden layer and a rectified linear unit (ReLU) activation function. The hidden layer is of 300 units in size, and in our investigation it is replaced by our TTL. The weight tensor $\mathcal{W} \in \mathbb{R}^{28 \times 28 \times 300}$ is in uncompressed format if its core $\mathcal{G} \in \mathbb{R}^{28 \times 28 \times 300}$. The compression factor (CF) is computed as the ratio of the number of elements of a “full” core tensor and factor matrices to the number of elements in a compressed core and its respective matrices. Table 3 shows results for different CFs, over a training period of 500 epochs.

The TTL achieved a compression factor (CF) of 18.73 with accuracy of 96.1%, and CF of 66.63 with accuracy of 94.6%, corresponding to a decrease of only less than 4% from the original uncompressed network. Figure 4 shows scatter plots of the normalized gradients $\frac{\partial L^*}{\partial \mathbf{U}^{(1)}}$ and $\frac{\partial L^*}{\partial \mathbf{U}^{(2)}}$, for both compression factors in Table 3. Observe that, for MNIST, both modes have comparable structural significance, as suggested by a simple visual perspective on the images (white numbers on black background).

7.4. Fashion-MNIST

We further evaluated our TTL model on the Fashion-MNIST dataset (Xiao et al., 2017), which is intended to serve as a direct, more complex replacement of the original MNIST. Fashion-MNIST consists of 28×28 greyscale images depicting fashion products belonging to a total of 10 different classes. The training and testing sets consist of 60000 and 10000 images, respectively. We employed a neural network

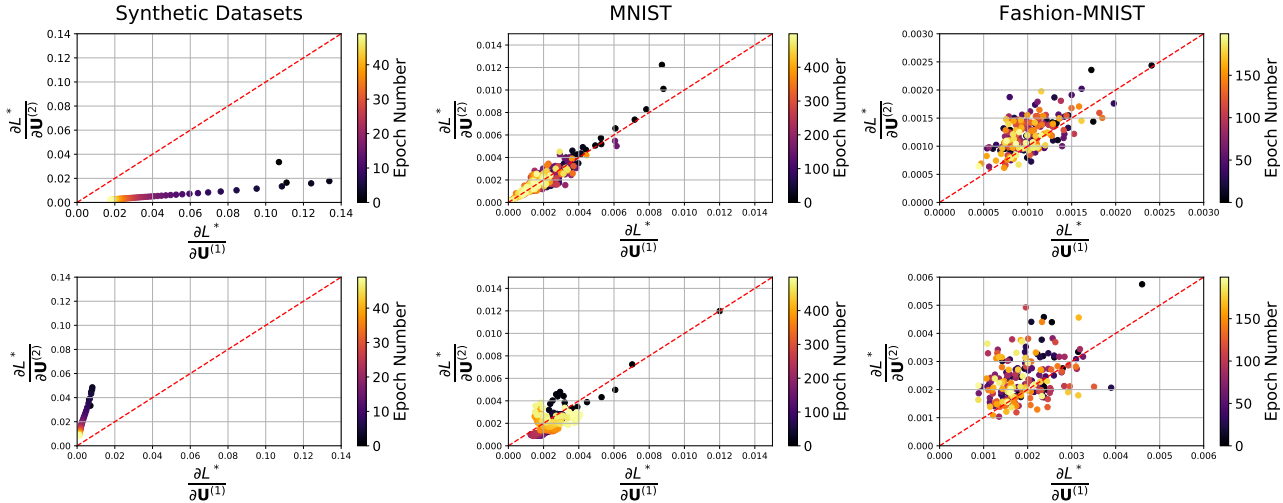


Figure 4: **Gradients across epochs – TTL applied to various datasets.** *Left column: Synthetic Datasets.* The top graph shows how gradients evolve during training for SD1, the bottom graph for SD2. The disparity in modal structural information is reflected in the magnitude of the normalized gradients. *Middle column: MNIST.* The top and bottom graphs show the evolution of the gradients when TTL with cores $\mathcal{G} \in \mathbb{R}^{10 \times 10 \times 30}$ and $\mathcal{G} \in \mathbb{R}^{5 \times 5 \times 10}$ are employed, respectively. No difference in modal structural information is observed. *Right column: Fashion-MNIST.* TTLs with $\mathcal{G} \in \mathbb{R}^{10 \times 10 \times 30}$ and $\mathcal{G} \in \mathbb{R}^{5 \times 5 \times 10}$ are used in the top and bottom graphs. Results suggest the second mode carries more structural information.

with 2 hidden layers of sizes 300 ($l = 1$) and 200 ($l = 2$), and ReLU activation functions. We replaced the layer $l = 1$ with our TTL. We compressed the layer by the same amount as for MNIST. The uncompressed network attained an accuracy of 83.2%, and, similarly as for MNIST, it lost less than 4% accuracy achieving a CF of 66.63, obtaining a 79.75% performance.

Differently from MNIST, Fashion-MNIST entails a disparity in modal structural information. For example, a coat and a dress occupy roughly the same vertical space on the images (we refer to (Xiao et al., 2017)), while the difference between the two products is revealed horizontally – mode-1 and mode-2. This disparity implies that mode-2 should play a relatively more important role than mode-1 in the training of the network. This is reflected in Figure 4, where it is shown that, on average, $\frac{\partial L^*}{\partial \mathbf{U}^{(2)}} > \frac{\partial L^*}{\partial \mathbf{U}^{(1)}}$. This further supports our arguments in Section 7.1, that each gradient $\frac{\partial L}{\partial \mathbf{U}^{(n)}}$ is directly intertwined with its corresponding mode- n , and some will be more informative about the training process depending on which data mode carries more structure. This is made explicit thanks to an analytical derivation of back-propagation, in terms of the TKD, which allowed us to leverage on, and gain insight from the expressive power of tensors.

8. Conclusions

We have introduced the Tucker Tensor Layer (TTL) as an alternative to the dense weight-matrices of fully connected

Table 3: **TTL performance for various Compression Factors (CF).**

Dataset	CF	Core Size	Accuracy (%)
MNIST	1	$28 \times 28 \times 300$	98.1%
	18.73	$10 \times 10 \times 30$	96.1%
	66.63	$5 \times 5 \times 10$	94.6%
Fashion MNIST	1	$28 \times 28 \times 300$	83.2%
	18.73	$10 \times 10 \times 30$	81.1%
	66.63	$5 \times 5 \times 10$	79.75%

layers in feed-forward Neural Networks (NNs). This has been achieved by treating the weight-matrix as the unfolding of a higher-order tensor and by decomposing it using the Tucker decomposition (TKD). By extending the notion of matrix derivatives to tensors, we have re-derived back-propagation within our proposed framework and have provided arguments for physical interpretability of our model. Experiments on synthetic data and on Fashion-MNIST show that, owing to the expressive power of tensors and in particular TKD, our framework has enabled us to gain insight into the network training process, by making explicit which data modes cover a more important role in training, thus mitigating the well-known black-box nature of NNs. The compressive benefits of our model have been demonstrated on both the MNIST and Fashion-MNIST datasets, with the TTL achieving a 66.63 fold compression while maintaining comparable performance to the uncompressed NN.

References

- Bro, Rasmus. PARAFAC. Tutorial and applications. *Chemometrics and Intelligent Laboratory Systems*, 38(2):149–171, 1997.
- Cao, Xingwei, Rabusseau, Guillaume, and Pineau, Joelle. Tensor regression networks with various low-rank tensor approximations. *arXiv preprint arXiv:1712.09520*, 2017.
- Cichocki, A., Mandic, D. P., Phan, A. H., Caiafa, C. F., Zhou, G., Zhao, Q., and Lathauwer, L. D. Tensor decompositions for signal processing applications. *IEEE Signal Processing Magazine*, 32(2):145–163, 2015.
- Cichocki, Andrzej, Lee, Namgil, Oseledets, Ivan, Phan, Anh-Huy, Zhao, Qibin, and Mandic, Danilo P. Tensor networks for dimensionality reduction and large-scale optimization: Part 1 Low-rank tensor decompositions. *Foundations and Trends in Machine Learning*, 9(4-5): 249–429, 2016.
- Graves, Alex, Mohamed, Abdel-rahman, and Hinton, Geoffrey. Speech recognition with deep recurrent neural networks. In *Proceedings of the IEEE International Conference on Acoustics, Speech and Signal Processing (ICASSP)*, pp. 6645–6649. IEEE, 2013.
- Kisil, Ilila, Moniri, Ahmad, Calvi, Giuseppe G., Scalzo Dees, Bruno, and Mandic, Danilo P. HOTTBOX: Higher Order Tensor ToolBOX. <https://github.com/hottbox>.
- Kolda, T.G. and Bader, B.W. Tensor decompositions and applications. *SIAM Review*, 51(3):455–500, 2009.
- Kossaifi, Jean, Lipton, Zachary C, Khanna, Aran, Furlanello, Tommaso, and Anandkumar, Anima. Tensor regression networks. *arXiv preprint arXiv:1707.08308*, 2(4), 2017.
- Krizhevsky, Alex, Sutskever, Ilya, and Hinton, Geoffrey E. Imagenet classification with deep convolutional neural networks. In *Proceedings of the Advances in Neural Information Processing Systems (NIPS)*, pp. 1097–1105, 2012.
- Lathauwer, L. De, Moor, B. De, and Vandewalle, J. A multilinear singular value decomposition. *SIAM Journal on Matrix Analysis and Applications*, 21(4):1253–1278, 2000.
- LeCun, Yann. The MNIST database of handwritten digits. <http://yann.lecun.com/exdb/mnist/>, 1998.
- LeCun, Yann, Bengio, Yoshua, and Hinton, Geoffrey. Deep learning. *Nature*, 521(7553):436, 2015.
- Magnus, Jan R and Neudecker, Heinz. Matrix Differential Calculus with Applications to Simple, Hadamard, and Kronecker Products. *Journal of Mathematical Psychology*, 29(4):474–492, 1985.
- Mandic, Danilo P. and Chambers, Jonathon. *Recurrent neural networks for prediction: learning algorithms, architectures and stability*. John Wiley & Sons, Inc., 2001.
- Novikov, Alexander, Podoprikin, Dmitrii, Osokin, Anton, and Vetrov, Dmitry P. Tensorizing neural networks. In *Proceedings of the Advances in Neural Information Processing Systems (NIPS)*, pp. 442–450, 2015.
- Oseledets, I. V. Tensor-train decomposition. *SIAM Journal on Scientific Computing*, 33(5):2295–2317, 2011.
- Rumelhart, David E, Hinton, Geoffrey E, and Williams, Ronald J. Learning representations by back-propagating errors. *Nature*, 323(6088):533, 1986.
- Russakovsky, Olga, Deng, Jia, Su, Hao, Krause, Jonathan, Satheesh, Sanjeev, Ma, Sean, Huang, Zhiheng, Karpathy, Andrej, Khosla, Aditya, Bernstein, Michael, et al. Imagenet large scale visual recognition challenge. *International Journal of Computer Vision*, 115(3):211–252, 2015.
- Simonyan, Karen and Zisserman, Andrew. Very deep convolutional networks for large-scale image recognition. *arXiv preprint arXiv:1409.1556*, 2014.
- Tucker, L. R. Implications of factor analysis of three-way matrices for measurement of change. In Harris, C. W. (ed.), *Problems in Measuring Change*, pp. 122–137. University of Wisconsin Press, Madison WI, 1963.
- Tucker, L. R. The extension of factor analysis to three-dimensional matrices. In Gulliksen, H. and Frederiksen, N. (eds.), *Contributions to Mathematical Psychology.*, pp. 110–127. Holt, Rinehart and Winston, New York, 1964.
- Xiao, Han, Rasul, Kashif, and Vollgraf, Roland. Fashion-MNIST: A novel image dataset for benchmarking machine learning algorithms. *arXiv preprint arXiv:1708.07747*, 2017.